



Assembly Level Topology Optimization Towards a Part Consolidation Algorithm for Additive Manufacturing

Luke Crispo¹ and Il Yong Kim²

Department of Mechanical and Materials Engineering, Queen's University, Kingston, Canada

As the adoption of additive manufacturing continues to grow in the aerospace industry, part consolidation is an emerging design technique aimed at decreasing assembly cost. Significant research is focused on design for additive manufacturing principles and their integration into design generation tools such as topology optimization, while part consolidation research has been limited to heuristic guidelines. This work presents the extension of topology optimization to assembly design for the simultaneous optimization of structural performance and connection layout. This methodology uses multiple domains occupying the same space along with a single joining domain to represent the assembly design. The proposed approach allows for future extensions with the calculation of additive manufacturing part costs on an individual domain level. The methodology is tested on a numerical example demonstrating the variation in part geometry and number of parts as the emphasis on joining cost is varied.

I. Introduction

The aerospace industry is rapidly embracing additive manufacturing (AM) as it enables the production of complex geometries that are cost-prohibitive or impossible to manufacture with subtractive or formative techniques. The increased part complexity that is realized from AM can improve performance and reduce cost of aerospace parts if the parts are redesigned for the new manufacturing process. Topology optimization, a computational tool that determines the ideal geometry of a part to maximize a specified objective, integrates easily with AM as the discretized results need little interpretation for manufacturability considerations. Research in AM has been geared towards the integration of AM constraints into topology optimization algorithms, mainly focusing on the reduction of support structure volume and small features [1-4].

The added design freedom gained from additive manufacturing allows for a reduction in the number of parts in an assembly, known as part consolidation (PC). The combination of several parts into a single design can reduce assembly cost and lead time [5] and can result in improved performance [6]. Research in PC has yielded a series of best practices and design rules for the consolidation design process [7-9] and a numerical algorithm to identify which parts of an assembly should be consolidated [10]. The consolidated part geometry is often redesigned manually after the candidates for consolidation have been selected, despite research stating that factors such as structural topology and build direction should be simultaneously optimized during redesign for improved structural performance of the part [11]. Oh et al reviewed assembly-based design literature for AM concluding that part decomposition (the splitting of a single part into an assembly) instead of part consolidation can improve process time, product quality, materials costs, and printability [12]. In a separate study, Oh et al outlines that there is a direct tradeoff between printing time and assembly time when selecting the number of parts in an assembly, and there is therefore an optimum number of parts that reduces the total processing time [13].

To integrate topology optimization and part consolidation, the traditional single part topology optimization approach must be extended for assembly design. Chickermane and Gea outlined an assembly level topology optimization approach using preselected design domain locations and a limited connection region with joints modelled

¹ M.A.Sc. Student, Department of Mechanical and Materials Engineering, Queen's University

² Professor, Department of Mechanical and Materials Engineering, Queen's University

using spring elements and their existence controlled by design variables [14]. In this study, the number of joints were constrained to a predefined value, with the part geometry and connection layout simultaneously optimized. Li et al determined optimal joint locations using evolutionary structural optimization to eliminate joints based on their structural efficiency from the applied loads [15]. Woischwill and Kim developed a multi-material multi-joint topology optimization technique to model the change in stiffness that occurs at connection interfaces and to account for this effect when optimizing a multi-material design [16]. This method was implemented in three dimensions along with added restrictions to joint types based on tooling accessibility constraints by Florea et al. [17].

Previous part consolidation research has focused on a top down consolidation approach, where parts of the original assembly are grouped together and subsequently redesigned. However, design freedom is restricted when part consolidation is based on a combination of the original parts in an assembly, meaning that it may result in a less optimal design or a reduction in performance. An alternative to the top down perspective is a bottom up approach that starts with the entire available design space of the assembly and divides it into parts. The bottom up method has an unlimited number of possible part combinations, removing the design restriction that occurs in a top down approach. Fig. 1 outlines the levels of part consolidation, where Levels 1 and 2 represent a top down approach while Level 3 is a bottom up redesign that is not constrained by the original assembly layout. This example shows how a clean slate design can realize a geometry that is not possible with standard top down approaches. Previous assembly-level topology optimization research falls under the Level 1 or Level 2 category as the individual domain locations are predefined during the problem definition.

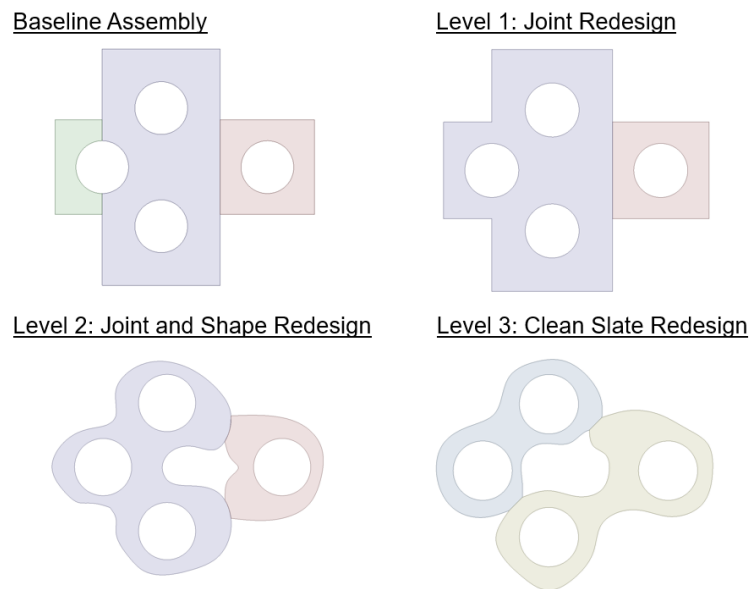


Fig. 1 Outline of the different levels of part consolidation with a depiction of possible consolidated designs for a hypothetical assembly.

The objective of this paper is to create a topology optimization algorithm capable of determining the ideal part geometry, number of parts, and connection design of an assembly. A bottom up approach will be applied to remove bias towards the initial assembly design. The proposed algorithm will model the structural performance and joining cost of an assembly and is designed for integration with additive manufacturing costs in future work. By considering all associated costs of an assembly, future algorithms will generate an optimized design based on the ratio between AM and assembly costs as well as the desired tradeoff between cost and performance.

II. Problem Formulation

Performing topology optimization on an assembly requires the development of a new approach for modelling multiple part geometries and the connections between those parts. The formulation of connections in this work are based on two key principles: 1) loads can only be transferred between two parts through a connection point, and 2) the stiffness of a connection is different from the stiffness of the surrounding material. The methodology proposed in this paper assumes a generic connection type and does not attempt to model the complex structural behavior at the joining location. The goal is instead to model the change in stiffness that occurs at a connection interface and to

consider this stiffness change when selecting joint locations. The actual connection interface will be refined after optimization based on the applicable best practices.

A. Assembly Level Topology Optimization

This paper proposes an assembly level topology optimization approach to model parts in L overlapping part domains each with identical design space geometry. Each part domain uses identical but disconnected finite element meshes (discretized into n elements) that are built on the design space of the original assembly. The separation of parts into individual domains is vital to future work as it allows for the selection of a unique build direction and calculation of support structure and build plate height uniquely for every part.

The topology of each part is specified by the vector of element densities χ with a length of $N = n * L$. Element densities are permitted to vary between 0 (representing a void) and 1 (representing material existence) while the elastic modulus of the element is calculated using the modified Solid Isotropic Material with Penalization (SIMP) approach [18] given by

$$E_e = E_e(x_e) = E_{\min} + x_e^p (E_0^1 - E_{\min}) \quad (1)$$

where E_e is the interpolated elastic modulus, x_e is the density of the e th element, p represents the penalization factor that discourages intermediate density, E_0^1 is the elastic modulus of the material, and E_{\min} is a small non-zero stiffness of void material.

In addition to the L layered part domains, a single joining domain is defined to determine the existence of connections between each part domain. This joining domain will allow connections to occur at all nodal locations within the design domain except for the exterior edges of the part. The existence of joints is specified in the vector y , with the strength of the connection varying continuously from 0 (representing no connection) to 1 (indicating a joint is present). A graphical representation of the design domains is outlined for a 2D geometry in Fig. 2, where each design domain is 2D plane. The planar domains are shown in Fig. 2A in an expanded view only for conceptualization and are all occupying the same space as shown in Fig. 2C. The concept is easily extended to three dimensions, where domains are instead overlapping cubes in 3D space.

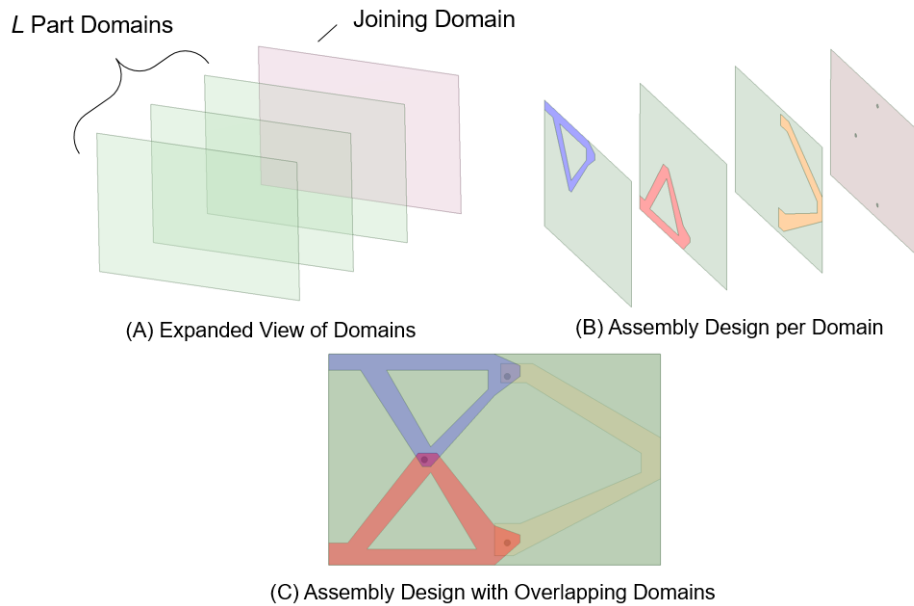


Fig. 2 Assembly level topology optimization approach visualized in two dimensions

Joints are structurally represented using a set of linear bar elements that connect degrees of freedom between part domains. The elastic modulus of the joint element is calculated as

$$E_j = E_j(y_j) = E_{\min} + y_j^q (E_0^2 - E_{\min}) \quad (2)$$

where E_j represents the stiffness and y_j represents the density of the j th joint, while q is the joint penalization factor, and E_0^2 is the joint elastic modulus. Note that the joint elastic modulus does not directly represent the elastic modulus of the joint material because the bar element has an arbitrary length. This value instead represents a joint stiffness that can be compared to element stiffness and can be adjusted based on the connection type.

If no rotational degrees of freedom are present in the model, connecting two domains together at a single node requires one bar element per spatial dimension. The stiffness matrix of a bar element is modified from the standard formulation by setting the cross-sectional area A , Young's Modulus E , and length l to a value of unity as the stiffness of the joint will be accounted for using the joint elastic modulus as calculated in Eq. (2). When considering a group of bar elements connecting between two domains, the stiffness matrix can be represented by the sum of the modified stiffness matrices as

$$\begin{bmatrix} \mathcal{K}_j^0 \end{bmatrix} = \begin{bmatrix} I & \cdots & -I \\ \vdots & \ddots & \vdots \\ -I & \cdots & I \end{bmatrix} \quad (3)$$

where \mathcal{K}_j^0 is the sub-joint stiffness matrix and I represents the identify matrix with a dimension equal to the number of spatial dimensions. The empty locations in this matrix are filled with zeros and represent all other degrees of freedom in the model that are unaffected by the connection. The sub-joint represents a set of bar elements that are used to connect only two domains at a single node. When more than two part domains are used in the model ($L > 2$), a single sub-joint is not sufficient to connect all domains together at a nodal location. In this scenario, sub-joints are placed from the domain with maximum element density to all other part domains, resulting in $L-1$ connections. This methodology ensures that there is never more than one load path between domains and that a load path will never pass through an empty domain. Connections are made to all domains, even those without element density, to allow for emerging density to develop in new locations during the optimization. After considering the placement of sub-joints, the joint stiffness at a single node location can be calculated as

$$\mathcal{K}_j = \sum_{i=1}^{L-1} (\mathcal{K}_j^0)_i \quad (4)$$

where \mathcal{K}_j represents the joint level stiffness matrix. The global level stiffness matrix of the entire assembly including all parts and joints can then be calculated as

$$K = \sum_{e=1}^N E_e(x_e) K_e^0 + \sum_{j=1}^M E_j(y_j) K_j \quad (5)$$

where K represents the global stiffness matrix of the assembly, K_e^0 is the element level stiffness matrix, and M represents the total number of possible joint locations.

The number of joints in the assembly, Γ , can be calculated as the sum of all joint densities as shown in Eq. (6). This value can be used to represent an approximate joining cost for the assembly. Note that all sub-joints at a single node are considered as a one connection. The parameter Γ does not represent the actual number of joints that would be needed to assemble the part as it is the sum of intermediate density finite joint elements. An interpretation of the optimization results would provide a more accurate assessment of the number and type of connections that would be needed in the assembly.

$$\Gamma = \sum_{j=1}^M y_j \quad (6)$$

B. Optimization Problem Statement

The assembly level topology optimization problem statement presented in (7) represents the foundation for future part consolidation algorithms. A multi-objective approach minimizes the weighted sum of compliance, C , and the

number of joints in the assembly, Γ , with w_1 representing the relative tradeoff between objectives that are normalized by initial objective function values C_0 and Γ_0 . The first constraint enforces the structural governing equation, with \underline{u} as the vector of nodal displacements and \underline{f} as the applied force. Material use is restricted using a volume fraction constraint where V_e represents the element volume, V_0 is the design space volume, and γ is the volume fraction limit.

$$\begin{aligned}
 \text{minimize : } J &= w_1 \frac{C(\underline{x}, \underline{y})}{C_0} + (1 - w_1) \frac{\Gamma(\underline{y})}{\Gamma_0} \\
 \text{subject to : } &\left(\sum_{e=1}^N E_e(x_e) K_e^0 + \sum_{j=1}^M E_j(y_j) K_j \right) \underline{u} = \underline{f} \\
 &\sum_{e=1}^N x_e V_e \leq \gamma V_0 \\
 &0 \leq x_e \leq 1 \quad \forall e \in \Omega \\
 &0 \leq y_j \leq 1 \quad \forall j \in \Omega \\
 &0 \leq w_1 \leq 1
 \end{aligned} \tag{7}$$

III. Problem Initialization

When performing topology optimization on a single part, forces are applied to the nodes specified in vector \underline{f} , while constraints are enforced by eliminating degrees of freedom from select nodes in the model. When solving a problem with multiple domains, the placement of forces and constraints is not obvious and can have a significant impact on the results. The placement of boundary conditions should not overly influence the convergence of the optimization towards any one assembly design. For example, placing the force and constrained nodes in different domains restricts design freedom as it requires at least two parts to transfer the load. The proposed algorithm splits the force between all part domains proportional to the ratio of density in each domain at the applied force node. For example, if there is even density in all domains then the force would be divided evenly; while if there is only density in one domain at the force location, the force would be applied to that domain only. After a specified number of iterations (3 in this work), the force is permanently placed in the domain with the largest density at that location. Constraints are applied to all domains because they do not enforce material use and a constraint surrounded by void elements does not significantly change the compliance of the resultant structure.

The initial element densities are typically set to the volume fraction defined in the compliance minimization problem statement. However, if all domains are identical in the initial iterations, there is no driving force to differentiate between domains because all element design variable sensitivities will be identical. Therefore, a unique element density distribution is needed to differentiate between domains, without overly dictating the geometry of the final design. For this work, smooth density gradients were applied to the initial domains with a high density originating in one end of the domain smoothly transitioning to a low density in the opposite side of the domain. Gradients are applied in opposing directions to a pair of domains to ensure that density is distributed evenly throughout the overall design domain. A sample gradient distribution for 2 domains is outlined in Fig. 3 showing a gradient distribution from the top to bottom of the domains.



Fig. 3 Sample initial density distribution with two domains using smooth gradients

IV. Results

The approach presented in this work was implemented in MATLAB using a modified version of the 88-line topology optimization code introduced by Andreassen et al [19]. The Helmholtz differential equation filter [20] along with the domain extension approach [21] was implemented to avoid checkerboarding and produce smooth optimization results. The optimization problem was solved using the method of moving asymptotes [22] with a convergence criteria of a 2% change in both objective functions over five iterations. An adaptive penalty scheme was used to refine the results, where the element penalization factor was initially set to $p = 3$ and incremented to 4 and later 5 after the convergence criteria were met. A bisection algorithm was used to threshold the optimized element densities while the joint densities were set to 0 or 1 based on a threshold value of 0.5.

The 2D Messerschmitt-Bolkow-Blohm (MBB) beam load case presented in Fig. 4 was used to test the proposed algorithm. The beam is discretized into 250×100 square elements of length of 1 with a Young's Modulus of $E_0^1 = 200$ GPa and a Poisson's ratio of $\nu = 0.3$ while the joint elastic modulus was set to $E_0^2 = 2$ GPa. Four part domains were used with initial density gradient distributions originating from the corners of each domain and the initial joint density was set to $y_0 = 0.15$.

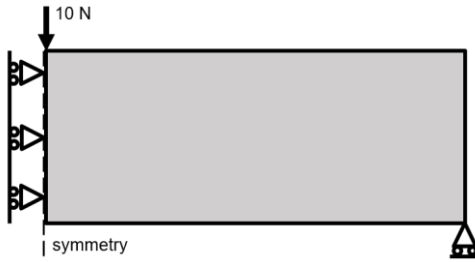


Fig. 4 Messerschmitt-Bolkow-Blohm (MBB) beam load case

With the material properties outlined in the problem, joints have 1% of the stiffness modulus compared to elements and significantly increase the compliance of the solution. It is therefore intuitive that an optimal solution which minimizes both joints and compliance should result in a single part without any joints. However, there are conflicting objective sensitivities for the joint design variables as objective sensitivities $dC/dy < 0$ and $d\Gamma/dy > 0$, meaning when the optimization is converging towards a multi-part design after the initial iterations, increasing the number of joints may reduce the objective function depending on the w_1 weighting.

The presented load case was optimized using the proposed methodology to minimize structural compliance and the number of joints subject to a volume fraction constraint of $\gamma = 0.3$. The weighting factor was varied from minimizing only compliance ($w_1 = 1$) to a large weighting on reducing joints ($w_1 = 0.2$). The results presented in Fig. 5 demonstrate that as w_1 increases, the optimization successfully reduces the number of joints and is capable of removing all joints from the assembly.

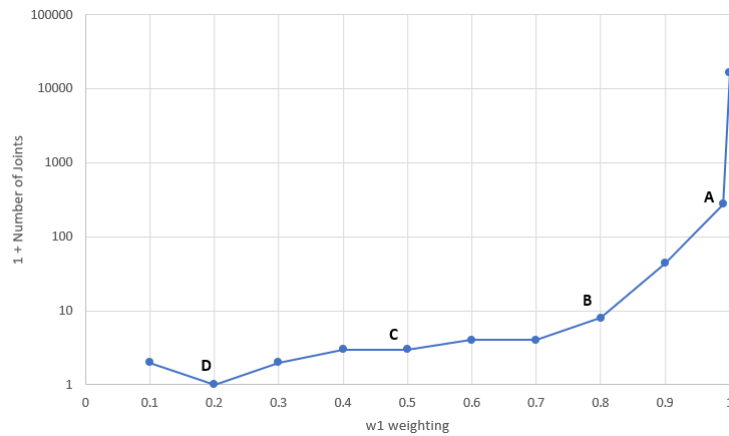


Fig. 5 Joint minimization of an MBB beam for varying weighting factors

Fig. 6 presents results for four w_1 weightings plotting all part and joint domains along with a combined domain to show the assembly design. Joints are plotted with a purple marker if the joint originates from that domain or a green marker if the joint originates from a different domain. These results show that minimizing joints also indirectly reduces the number of parts in the assembly. As the weighting factor is varied, the optimization provides solutions ranging from a single part to seven parts.

Compliance values are also displayed in Fig. 6 and confirm that a single assembly design provides the best solution for both objective functions. These results demonstrate that the proposed joint minimization approach can reduce the number of parts in the assembly by changing only the weighting factor. This is crucial for future work where part cost factors will be considered in the multi-objective approach and an array of optimal solutions will exist depending on the trade-off between joining and part costs.

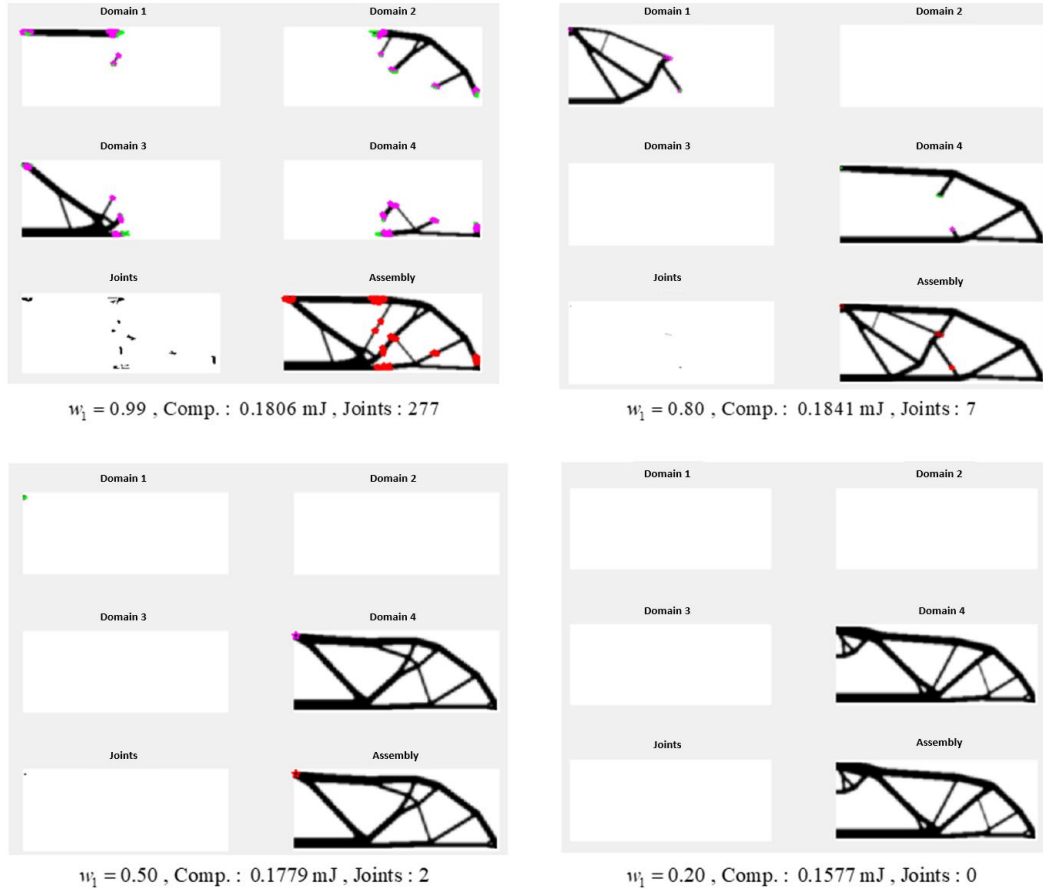


Fig. 6 Optimization results for MBB load case with joint and compliance minimization

V. Conclusion

This paper proposes an assembly level topology optimization formulation that models multiple parts in overlapping design domains accompanied by a single joining domain that identifies the connections between each part. The bottom up approach to part consolidation removes any bias to the original assembly geometry resulting in improved design freedom allowing for designs that are not possible with top-down methods. The multi-objective optimization problem statement minimizes both structural performance and joining cost based on a specified weighting factor. The initialization of element densities and applied forces is discussed, and a proposed method is implemented to encourage unique geometry in each domain without overly influencing the assembly design. Application of the methodology to an MBB beam load case indicated that the algorithm can produce a range of consolidated designs with varied weighting factors between structural performance and joining cost. The implementation of additive manufacturing constraints into the optimization problem statement will allow future algorithms to determine the ideal number of parts based on the tradeoffs in AM and assembly costs. The extension of the methodology into 3D and implementation with complex geometry is needed to solve real world problems.

References

- [1] L. Ryan, and I. Y. Kim, "A multiobjective topology optimization approach for cost and time minimization in additive manufacturing," *International Journal for Numerical Methods in Engineering*, Vol. 118, No. 7, May. 2019, pp. 371-394.
doi: 10.1002/nme.6017
- [2] G. Sabiston, and I. Y. Kim, "3D topology optimization for cost and time minimization in additive manufacturing," *Structural Multidisciplinary Optimization*, 22 Oct. 2019.
doi: 10.1007/s00158-019-02392-7
- [3] J. K. Liu, et al., "Current and future trends in topology optimization for additive manufacturing," *Structural and Multidisciplinary Optimization*, Vol. 57, No. 6, Jun. 2018, pp. 2457-2483.
doi: 10.1007/s00158-018-1994-3
- [4] R. Ranjan, R. Samant, and S. Anand, "Integration of Design for Manufacturing Methods With Topology Optimization in Additive Manufacturing," *Journal of Manufacturing Science and Engineering*, Vol. 139, No. 6, Jun. 2017.
doi: 10.1115/1.4035216
- [5] A. Stevenson, M. Baumers, J. Segal, and S. Macdonell, "How Significant Is the Cost Impact of Part Consolidation," *Solid Freeform Fabrication Symposium*, 2017, pp. 2551-2562.
- [6] J. Schmelzle, E. V. Kline, C. J. Dickman, E. W. Reutzel, G. Jones, and T. W. Simpson, "(Re)Designing for Part Consolidation: Understanding the Challenges of Metal Additive Manufacturing," *Journal of Mechanical Design*, Vol. 137, No. 11, Nov. 2015.
doi: 10.1115/1.4031156
- [7] H. Rodrigue, and M. Rivette, "An assembly-level design for additive manufacturing methodology," *IDMME-Virtual Concept*, France, 2010.
- [8] G. Sossou, F. Demoly, G. Montavon, and S. Gomes, "An additive manufacturing oriented design approach to mechanical assemblies," *Journal of Computational Design and Engineering*, Vol. 5, No. 1, Jan. 2018, pp. 3-18.
doi: 10.1016/j.jcde.2017.11.005
- [9] S. Yang, and Y. F. Zhao, "Additive Manufacturing-Enabled Part Count Reduction: A Lifecycle Perspective," *Journal of Mechanical Design*, Vol. 140, No. 3, Mar. 2018.
doi: 10.1115/1.4038922
- [10] S. Yang, F. Santoro, and Y. F. Zhao, "Towards a Numerical Approach of Finding Candidates for Additive Manufacturing-Enabled Part Consolidation," *Journal of Mechanical Design*, Vol. 140, No. 4, Apr. 2018.
doi: 10.1115/1.4038923
- [11] J. K. Liu, "Guidelines for AM part consolidation," *Virtual and Physical Prototyping*, Vol. 11, No. 2, 2016, pp. 133-141.
doi: 10.1080/17452759.2016.1175154
- [12] Y. Oh, C. Zhou, and S. Behdad, "Part decomposition and assembly-based (Re) design for additive manufacturing: A review," *Additive Manufacturing*, Vol. 22, Aug. 2018, pp. 230-242.
doi: 10.1016/j.addma.2018.04.018
- [13] Y. Oh, S. Behdad, and C. Zhou, "Part Separation Methods for Assembly Based Design in Additive Manufacturing," *Proceedings of the Asme International Design Engineering Technical Conferences and Computers and Information in Engineering Conference*, Vol. 4, 2017.
- [14] H. Chickermane, and H. C. Gea, "Design of multi-component structural systems for optimal layout topology and joint locations," *Engineering with Computers*, Vol. 13, No. 4, 1997, pp. 235-243.
doi: 10.1007/Bf01200050
- [15] Q. Li, G. P. Steven, and Y. M. Xie, "Evolutionary structural optimization for connection topology design of multi-component systems," *Engineering Computations*, Vol. 18, No. 3-4, 2001, pp. 460-479.
doi: 10.1108/02644400110387127
- [16] C. Woischwill, and I. Y. Kim, "Multimaterial multijoint topology optimization," *International Journal for Numerical Methods in Engineering*, Vol. 115, No. 13, Sep 28. 2018, pp. 1552-1579.
doi: 10.1002/nme.5908
- [17] V. Florea, M. Pamwar, B. Sangha, and I. Y. Kim, "3D multi-material and multi-joint topology optimization with tooling accessibility constraints," *Structural and Multidisciplinary Optimization*, July 17. 2019.
doi: 10.1007/s00158-019-02344-1

- [18] O. Sigmund, "Morphology-based black and white filters for topology optimization," *Structural and Multidisciplinary Optimization*, Vol. 33, No. 4-5, Apr. 2007, pp. 401-424.
doi: 10.1007/s00158-006-0087-x
- [19] E. Andreassen, A. Clausen, M. Schevenels, B. S. Lazarov, and O. Sigmund, "Efficient topology optimization in MATLAB using 88 lines of code," *Structural and Multidisciplinary Optimization*, Vol. 43, No. 1, Jan. 2011, pp. 1-16.
doi: 10.1007/s00158-010-0594-7
- [20] B. S. Lazarov, and O. Sigmund, "Filters in topology optimization based on Helmholtz-type differential equations," *International Journal for Numerical Methods in Engineering*, Vol. 86, No. 6, May. 2011, pp. 765-781.
doi: 10.1002/nme.3072
- [21] A. Clausen, and E. Andreassen, "On filter boundary conditions in topology optimization," *Structural and Multidisciplinary Optimization*, Vol. 56, No. 5, Nov. 2017, pp. 1147-1155.
doi: 10.1007/s00158-017-1709-1
- [22] K. Svanberg, "The Method of Moving Asymptotes - a New Method for Structural Optimization," *International Journal for Numerical Methods in Engineering*, Vol. 24, No. 2, Feb. 1987, pp. 359-373.
doi: 10.1002/nme.1620240207